

# Population transfer in a Lambda system induced by detunings

P.G. Di Stefano,<sup>1</sup> E. Paladino,<sup>1,2,3</sup> A. D'Arrigo,<sup>1,2</sup> and G. Falci<sup>1,2,3,\*</sup>

<sup>1</sup>*Dipartimento di Fisica e Astronomia, Università di Catania, Via Santa Sofia 64, 95123 Catania, Italy.*

<sup>2</sup>*CNR-IMM UOS Università (MATIS), Consiglio Nazionale delle Ricerche, Via Santa Sofia 64, 95123 Catania, Italy.*

<sup>3</sup>*Istituto Nazionale di Fisica Nucleare, Via Santa Sofia 64, 95123 Catania, Italy.*

(Dated: February 19, 2022)

In this paper we propose a new protocol to achieve coherent population transfer between two states in a three-level atom by using two ac fields. It is based on the physics of Stimulated Raman Adiabatic Passage (STIRAP), but it is implemented with the constraint of a reduced control, namely one of the fields cannot be switched off. A combination of frequency chirps is used with resonant fields, allowing to achieve approximate destructive interference, despite of the fact that an exact dark state does not exist. This new chirped STIRAP protocol is tailored for applications to artificial atoms, where architectures with several elementary units can be strongly coupled but where the possibility of switching on and off such couplings is often very limited. Demonstration of this protocol would be a benchmark for the implementation of a class of multilevel advanced control procedures for quantum computation and microwave quantum photonics in artificial atoms.

PACS numbers: 03.67.Lx, 85.25.-j, 03.65.Yz

## I. INTRODUCTION

Preparation of a quantum system in a well defined state is an essential task in many branches of modern physics ranging from atomic and molecular physics<sup>1</sup> to quantum computation<sup>2</sup>. Techniques for transferring population from a ground state  $|0\rangle$  to a state  $|1\rangle$  employ either Rabi cycling or adiabatic passage (AP)<sup>3</sup>. Amongst these latter STIRAP is a three-level atom scheme where selective and faithful population transfer is achieved by operating with two resonant driving fields in  $\Lambda$  configuration<sup>3,4</sup>. The advantage over Rabi cycling is the dramatic reduction of sensitivity to fluctuations of the parameters, at the expenses of a longer duration of the adiabatic protocol. In more complex architectures semiclassical driving fields are substituted by harmonic modes of a strongly coupled cavity, and tasks as preparation of photons with controlled amplitude, frequency and polarization<sup>5,6</sup> can be performed by vacuum-stimulated Raman AP (vSTIRAP).

In the last few years multilevel coherence in solid-state systems, from mesoscopic devices<sup>7</sup> to atomic-like impurity states<sup>8</sup>, has been a fertile subject of investigation. In particular superconducting-based “artificial atoms”<sup>9–11</sup> are very promising since coherent phenomena proper of the mesoscopic realm have been demonstrated on the mesoscopic scale. With respect to their natural counterpart, artificial atoms offer the advantage that composite structures can be fabricated on a single chip<sup>12</sup>, which allows manipulation of single photons at GHz frequencies opening the new scenario of microwave quantum photonics<sup>13</sup>. Moreover new architectures could be implemented with both larger couplings<sup>14</sup> and a larger degree of integration than their atomic counterparts.

In the last few years several theoretical proposals<sup>15–21</sup> and experiments<sup>22–25</sup> have dealt with multilevel coherence in artificial atoms. Distinctive features of such systems are the effectiveness of parity selection rules<sup>16,18,21</sup>

which together with the presence of strong  $1/f$  noise<sup>26,27</sup>, impose constraints on the available control. Therefore new protocols for manipulating the coherent dynamics must be tailored for such systems. Their design requires that large couplings allowing for efficient control are combined with protection from noise<sup>21</sup>.

In this paper we present a new protocol to achieve coherent population transfer between the two lowest excited states of a three-level atom by using two ac fields. The key difference with standard STIRAP, where ac fields must be switched on and off in a counterintuitive sequence<sup>4</sup>, is that one of the fields is kept always-on, its amplitude being constant during the protocol. Operations require phase modulation, and for this reason we call the protocol cSTIRAP (chirped STIRAP). Sweeping the frequency of a single classical driving field across the resonance is a standard way to switch on and off Rabi oscillations, thereby one may think to rephrase STIRAP accordingly, but this is not the case. Indeed coherent population requires destructive interference of the two fields<sup>28</sup>. This is guaranteed by cSTIRAP, which thereby solves a non-trivial control problem, its experimental demonstration in artificial atoms being by itself an important proof of principle of advanced three-level control. Even more interestingly, cSTIRAP could apply to architectures where “artificial atoms” are coupled to quantized modes, electromagnetic or nanomechanical, where strong coupling is achieved by non-switchable hardware elements keeping the interaction always-on. The protocol we propose possesses certain advantageous distinctive characteristics: (i) it works with reduced available control, as always-on field, (ii) it operates with nearly resonant fields, reducing the operation time; (iii) it may rely on better techniques to control the phase of microwave circuits, (iv) it is cyclic.

The paper is organized as follows. In Sec.II we introduce the model Hamiltonian and briefly review standard implementations of coherent population transfer in

two and three-level atoms. In Sec. III we illustrate the new protocol discussing in Sec. IV the robustness against parametric fluctuations and in Sec. V decoherence effects. Finally, in Sec. VI, along with the conclusions, we will discuss the comparison of cSTIRAP with other protocols for population transfer operated by frequency chirps.

## II. COHERENT POPULATION TRANSFER IN LAMBDA ATOMS

In two-level systems coherent population transfer  $|0\rangle \rightarrow |1\rangle$  by AP is performed by shining a direct coupling field whose detuning is swept through the resonance at the Bohr frequency of the transition. Common examples are Rapid AP (RAP) or Stark Chirped RAP (SCRAP)<sup>1</sup>.

In three-level systems population transfer may be achieved in absence of direct coupling, via a third *linkage* state  $|2\rangle$ , coupled to  $|0\rangle$  and  $|1\rangle$  by a pump field at frequency  $\omega_p \simeq E_2 - E_0$  and a Stokes field at  $\omega_s \simeq E_2 - E_1$ , respectively. In particular the *Lambda configuration* depicted in the top inset of Fig. 1 will be considered in this work. Since  $|2\rangle$  is usually short-lived, one of the goals of coherent techniques is to use  $|2\rangle$  but *never populate it*. This is achieved in a very efficient and elegant way relying on destructive interference<sup>28</sup>. The Hamiltonian in the rotating wave approximation, in the basis of the bare states  $\{|0\rangle, |1\rangle, |2\rangle\}$ , is expressed in a doubly rotating frame as

$$H = \begin{bmatrix} 0 & 0 & \frac{1}{2}\Omega_p^*(t) \\ 0 & \delta(t) & \frac{1}{2}\Omega_s^*(t) \\ \frac{1}{2}\Omega_p(t) & \frac{1}{2}\Omega_s(t) & \delta_p(t) \end{bmatrix} \quad (1)$$

where  $\Omega_k(t)$  with  $k = p, s$  are the Rabi frequencies of the pump and the Stokes fields, which are detuned by  $\delta_p := E_2 - E_0 - \omega_p$  and  $\delta_s := E_2 - E_1 - \omega_s$  respectively. A key quantity is the two-photon detuning, defined as  $\delta := \delta_p - \delta_s$ .

Conventional STIRAP relies on the fact that at two-photon resonance,  $\delta(t) = 0$ , an instantaneous eigenvector with zero eigenvalue  $\epsilon_0 = 0$  exists given by

$$|D(t)\rangle = \frac{\Omega_s(t)|0\rangle - \Omega_p(t)|1\rangle}{\sqrt{\Omega_s^2(t) + \Omega_p^2(t)}} \quad (2)$$

It is called *dark state* since population is confined in the “trapped subspace”  $\{|0\rangle, |1\rangle\}$ , despite of the fact that the two fields excite both the  $0 \rightarrow 2$  and the  $1 \rightarrow 2$  transitions. The key phenomenon preventing population of  $|2\rangle$  is destructive interference between the amplitudes corresponding to the two absorption patterns<sup>1,28</sup>. Conventional STIRAP consists in letting the dark state evolve adiabatically from  $|D(-\infty)\rangle = |0\rangle$  to  $|D(\infty)\rangle = |1\rangle$ . This is achieved by shining pulses  $\Omega_k(t)$  in a “counterintuitive” sequence, the Stokes at first and then the pump. An important characteristic of STIRAP is the fact that AP is operated when both fields are on, determining a

two-photon effective coupling  $|0\rangle \leftrightarrow |1\rangle$ . STIRAP has been observed in a variety of physical systems<sup>3,4</sup>. The two-photon character of population transfer, and the fact that the protocol is maximally efficient with fully resonant fields,  $\delta = \delta_s = \delta_p = 0$  is the key for interesting applications with quantized fields.

Another three-level technique, Raman Chirped Adiabatic Passage (RCAP)<sup>29</sup>, uses instead phase modulation. Population transfer is achieved by two far off-resonance chirped laser pulse sweeping through resonance (see Sec. VI). Unlike conventional STIRAP, two-photon resonance is not kept during the whole process, causing a transient population of state  $|2\rangle$  to appear. The latter in principle can be made small by accurate tuning of parameters.

## III. COHERENT POPULATION TRANSFER WITH AN ALWAYS-ON FIELD

In this section we will address the problem of achieving  $|0\rangle \rightarrow |1\rangle$  population transfer subject to two constraints, namely (a) keeping the population of  $|2\rangle$  small and (b) operating with a reduced control, in particular with one of the fields, for instance the Stokes one, kept always on,  $\Omega_s(t) =: \Omega_0 \neq 0$ . Naively one could suppose that sweeping the detuning  $\delta_s(t)$  could allow to effectively switch on and off  $\Omega_s$ , allowing again for conventional STIRAP. However this is not the case because coherent population transfer requires that the two-photon resonance condition,  $\delta = 0$ , is kept while sweeping  $\delta_s(t)$ , to ensure destructive interference. In what follows we will seek for a solution allowing to achieve complete population transfer by properly shaping the detunings.

First of all when one of the fields is always on, the Hamiltonian (1) for  $t \rightarrow \pm\infty$  is not diagonal in the bare state basis. In order to approximate asymptotically the desired target state  $|1\rangle$ , necessarily at the end of the protocol we must have  $\delta_s \gg \Omega_0$ . If we take detunings shaped as shown in Fig.1, which are given by

$$\begin{aligned} \delta_s(t) &= \frac{1}{2} h_\delta \Omega_0 \left[ \tanh\left(\frac{t - \tau}{\tau_{ch}}\right) + \tanh\left(\frac{t + \tau}{\tau_{ch}}\right) \right] \\ \delta_p(t) &= \kappa_\delta \delta_s(t) \end{aligned} \quad (3)$$

the desired asymptotics is ensured by  $h_\delta \gg 1$ , i.e. the protocol must start and end with “far detuned” lasers. The modulation (3) has the important characteristics that at least for part of the protocol  $\delta(t) = 0$  (Fig. 1). During this phase a Stokes-induced Autler-Townes (AT) splitting opens. Although an exact adiabatic dark state is not available for population transfer, we will argue later that keeping  $\delta \approx 0$  allows to minimize the transient population of  $|2\rangle$ .

The population transfer mechanism is better understood studying the evolution of the instantaneous eigenvalues and eigenvectors of the “Stokes” Hamiltonian, ob-

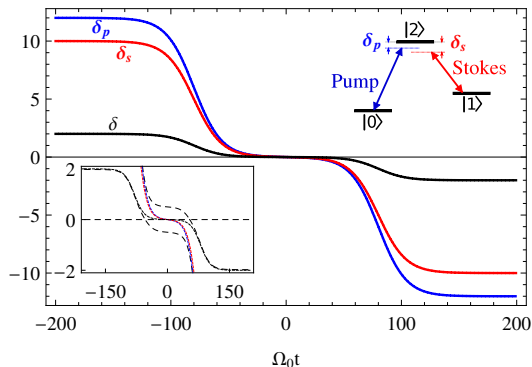


FIG. 1. (color online) Main figure: single (coloured lines) and two-photon (dotted line) detunings in  $\Omega_0$  units. Top inset: Three level Lambda system. Bottom inset: Zoom of the single and two-photon detunings (solid lines), plotted together with the Stokes eigenvalues (dashed lines) of Eq. (6) showing the appearance of a dynamical Stokes-induced AT, which is switched on and off by modulation of  $\delta_s$ .

tained setting to zero the pump field in Eq.(1)

$$H_s(t) = \begin{bmatrix} 0 & 0 & 0 \\ 0 & \delta(t) & \frac{1}{2}\Omega_0 \\ 0 & \frac{1}{2}\Omega_0 & \delta_p(t) \end{bmatrix} \quad (4)$$

Here the Rabi frequency has been taken real with no loss of generality. The Stokes Hamiltonian acts non-trivially only on the  $\{|1\rangle, |2\rangle\}$  subspace, yielding the asymptotic states

$$\begin{aligned} |s_+( -\infty )\rangle &\simeq |2\rangle \rightarrow |s_+( +\infty )\rangle \simeq |1\rangle \\ |s_-( -\infty )\rangle &\simeq |1\rangle \rightarrow |s_-( +\infty )\rangle \simeq |2\rangle \end{aligned} \quad (5)$$

The "Stokes eigenvalues" display the presence of the AT splitting during the protocol (Fig. 1, bottom inset)

$$s_0 = 0, \quad s_{\pm} = \delta + \frac{\delta_s \pm \sqrt{\delta_s^2 + \Omega_0^2}}{2} \quad (6)$$

During this AT phase  $\delta_s$  is swept across the resonance swapping  $|1\rangle \leftrightarrow |2\rangle$ .

Using detunings Eq.(3) with  $\kappa_\delta > 1$  the pattern of split instantaneous eigenvalues  $s_{\pm}(t)$  is crossed twice by the eigenvalue  $s_0 = 0$ , as shown in Fig. 2(a). Crossings occur at times  $\pm t_c$  when  $s_{\pm}(t) = 0$ , i.e.  $4\delta(t_c)\delta_p(t_c) = \Omega_0^2$ . In these conditions the system prepared in  $|\psi(-\infty)\rangle = |0\rangle$  remains of course in this state, passing through the crossing. Population transfer is achieved by applying a pump pulse with finite area reaching its peak value close to the second crossing,  $t = t_c$ . For instance, employing a Gaussian pulse, we have

$$\Omega_p(t) = \kappa \Omega_0 e^{-\left(\frac{t-t_c}{T}\right)^2} \quad (7)$$

The behavior is understood in terms of the instantaneous eigenenergies of the full Hamiltonian Eq. (1). In particular the pump pulse lifts the degeneracy between

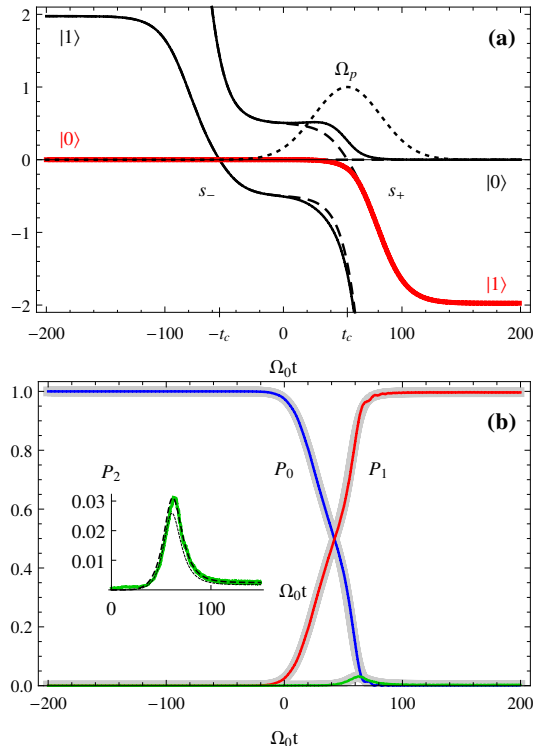


FIG. 2. (color online) (a) Eigenvalues of the Stokes Hamiltonian of Eq. (4) (dashed lines) and of the full Hamiltonian of Eq. (1) (solid lines) in  $\Omega_0$  units. The red thick line is the instantaneous energy of the system adiabatically driven from  $|0\rangle$  to  $|s_+\rangle \simeq |1\rangle$  through the opening of the avoided crossing generated by the pump pulse (dotted line) at time  $t = t_c$ . (b) Population histories (red, blue and green lines) from the numerical solution of the Schrödinger equation, for  $\Omega_s(t) = \Omega_0$ ,  $\Omega_0 T = 40$ ,  $h_\delta = 10$ ,  $\kappa_\delta = 1.2$  and  $\kappa = 1$ ,  $\tau_{ch} = 0.6T$ , showing complete population transfer by cSTIRAP. For these parameters the adiabatic approximation (gray curves) fully agrees with the exact solution. Inset: the exact population  $P_2$  of the excited state (green solid line) is small at any time of the protocol, as can be estimated by Eq.(8) (thin line). The dashed line refers to the approximation of Eq. (A4).

$s_0$  and  $s_+$  turning their crossing into an avoided crossing [Fig.2(a)]. The adiabatic connection corresponding to  $s_+$  yields eventually the desired population transfer,  $|0\rangle \rightarrow |s_+(+\infty)\rangle \simeq |1\rangle$ .

We remark that population transfer depends only on the presence of a crossing between Stokes eigenenergies  $s_+$  and  $s_0$  and on the fact that the adiabatic approximation is valid. In this regime the precise shape of the pulses is not relevant. Therefore the protocol is robust against imperfections in the control. From the physical point of view it is worth stressing that the pump pulse triggers AP by a two-photon process. The distinctive feature of our proposal is that this two-photon effective coupling is obtained with both quasi resonant pump and Stokes fields. This ensures large efficiency for rather small pulse duration. We mention that during its switching on  $\Omega_p$

could in principle trigger unwanted transitions  $|0\rangle \rightarrow |2\rangle$ , which are however suppressed by the Stokes-induced AT splitting and the two-photon resonance condition. A similar phenomenon occurs in standard STIRAP, where it is called the Stokes-induced EIT (electromagnetically induced transparency) phase<sup>3</sup>.

Summing up cSTIRAP can be described in the language of Ref. 3 as a five stages protocol, with successive far-detuned, Stokes-induced AT, Stokes-induced EIT, two-photon AP and again far-detuned phases. In what follows we will see that the other important requirement, namely that population of  $|2\rangle$  should be minimal at all times, is also fulfilled. This requirement is necessary in order to prevent unwanted decay processes likely to occur in real physical systems, where  $|2\rangle$  is often unstable.

We estimate  $P_2 = |\langle 2|\psi\rangle|^2$  by adiabatic elimination. The standard procedure formulated in the bare basis yields the state  $|\psi_{AE}^0\rangle = c_0|0\rangle + c_1|1\rangle$  (see App. A). First order corrections yield a leakage from the subspace  $\{|0\rangle, |1\rangle\}$  given by<sup>29</sup>

$$P_2(t) \simeq \left| \frac{\Omega_p c_0 + \Omega_0 c_1}{2\delta_p} \right|^2 \quad (8)$$

that can be made very small, as shown in Fig.2(b), which also shows that this approximation works very well. A better approximation is obtained by working in the Stokes basis [see App. A and Fig. 2(b)], but Eq.(8) has a simpler analytic form, allowing to write a figure of merit for the parametric dependence of leakage during the protocol. A simple choice is to consider leakage at the crossing  $s_+ = 0$

$$P_2(t_c) \simeq \frac{\delta}{\delta_p} f(\kappa) = \frac{\kappa_\delta - 1}{\kappa_\delta} f(\kappa) \quad (9)$$

Here  $f(\kappa)$  is a monotonically decreasing function of the ratio of the Rabi peak amplitudes  $\kappa$ . This qualitative behaviour is confirmed by numerical simulations shown in Fig. 3, where the efficiency is plotted versus relative magnitude of the amplitudes ( $\kappa$ , left panel) and of the detunings ( $\kappa_\delta$ , right panel), both in the absence (top panel) and in the presence (bottom panel) of a finite lifetime  $\tau_2 = T/2$  of the intermediate state  $|2\rangle$  (see section IV for a model). It is seen that efficiency increases with increasing  $\kappa$  as an effect of a larger avoided crossing at  $s_+ = 0$ . Moreover increasing  $\kappa$  reduces the transient population of  $|2\rangle$ , as given by the figure of merit Eq.(9). This is seen by comparing the insets of the left panels of Fig. 3: the positive slope of the sensitivity in the presence of a finite  $\tau_2$  [Fig. 3(c)] cannot be explained as an improvement in adiabaticity, since this slope is not present in the ideal case [Fig. 3(a)]. Therefore, it can only be caused by a reduction of  $P_2$ . Population transfer occurs only for  $\kappa_\delta > 1$  as shown in Fig. 3(b),(d). In particular, for  $\kappa_\delta = 1$  we have  $\delta(t) = 0$  and Eq.(2) applies, showing that an always on Stokes field would produce a return of the population to the initial state. For  $\kappa_\delta < 1$  the Stokes

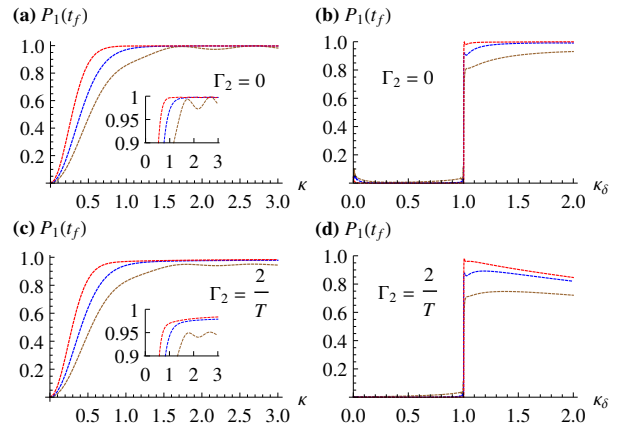


FIG. 3. (color online) Upper panels: STIRAP efficiency vs the relative peak amplitudes of the fields (left panel, where  $\kappa_\delta = 1.2$ ) and to the relative detunings (right panel, where  $\kappa = 1$ ), for various degrees of adiabaticity (curves:  $\Omega_0 T = 40$  (red), 20 (blue), 10 (brown) from higher to lower efficiency). For  $\kappa_\delta > 1$ , and provided adiabaticity is good, the system has a very slight sensitivity to these parameters. Lower panels: sensitivity of the efficiency to unwanted transient population of  $|2\rangle$  accounted for by a finite lifetime  $\tau_2 = 1/\Gamma_2$  (cf. Eq.10). The insets of panels (a) and (c) are zooms of the corresponding main figures showing how, in the presence of a non-vanishing  $\Gamma_2$ , the efficiency improves with increasing  $\kappa$ .

eigenvalues do not cross, and adiabatic dynamics leads to a final population entirely in  $|0\rangle$ .

#### IV. SENSITIVITY TO PARAMETERS

The efficiency of cSTIRAP is not very sensitive to slight deviations of relative amplitudes  $\kappa$  and detunings  $\kappa_\delta$  of the pulses, provided adiabaticity is kept. This is shown in Fig. 3, results in the lower panels allowing to fix convenient values  $\kappa = 1$ ,  $\kappa_\delta = 1.2$  and  $\Omega_0 T = 40$ , which we will use hereafter.

As in conventional STIRAP<sup>3</sup>, the most critical feature is the parametric sensitivity to stray detunings. Here we discuss this issue, which is also responsible for decoherence due to low-frequency noise<sup>21,27</sup>.

The physics is understood recalling the picture of conventional STIRAP, where two kind of errors emerge<sup>1</sup>. “Bad projection” errors, due a bad choice of the pulse shape and timing, may lead to the wrong target state. “Bad adiabaticity” errors induce leakage from the trapped subspace, nonadiabatic transitions surely occurring when the so called “global condition”  $\Omega_k T \gg 1$  is not met. Both kinds of errors are also triggered by fluctuations induced by an environment (see Sec.V). For cSTIRAP we verified that large enough  $\Omega_k T$  again guarantees adiabaticity (Fig. 3). In this regime a strong asset of cSTIRAP is that it is not affected by bad projection errors in the far-detuned phases, since final eigenstates in the rotating frame are nondegenerate.

However since the efficiency of cSTIRAP depends on the structure of crossings of the eigenvalues of the Stokes Hamiltonian, it may be affected by stray detunings during the protocol. A further drawback comes from the fact that the state carrying population in cSTIRAP, while taking advantage from destructive interference, it is not an exact dark state as in Eq.(2), since the condition  $\delta(t) = 0$  does not hold true. This is a potentially important source of error for cSTIRAP since it also may determine a nonvanishing population of  $|2\rangle$  at intermediate times. Sensitivity to detunings is conveniently studied by the non-Hermitian Hamiltonian:

$$H(t|\{\delta_k\}) \rightarrow H(t|\{\delta_k\}) + i\Gamma_2|2\rangle\langle 2| \quad (10)$$

Using a sufficiently large  $\Gamma_2 > 1/T$  guarantees that transient population of  $|2\rangle$  decays elsewhere (e.g. in a continuum), yielding a lack of normalization at the end of the protocol. Therefore the resulting efficiency  $P_1(t_f)$  is a figure of merit embedding the requirement that  $|2\rangle$  should be never populated.

The Hamiltonian (10), where only the dependence on detunings is emphasized, accounts for the effect of stray components by letting

$$\begin{aligned} \delta_k(t) &\rightarrow \delta_k(t) + \tilde{\delta}_k, \quad k = s, p \\ \delta(t) &\rightarrow \delta(t) + \tilde{\delta}, \quad \tilde{\delta} := \tilde{\delta}_p - \tilde{\delta}_s \end{aligned} \quad (11)$$

Stray detunings may describe very slow phase fluctuations (at frequencies  $\ll 1/T$ ) of the driving fields. Physically in solid-state devices they describe energy fluctuations due to coupling to an environment (see Sec.V and Ref. 21) whose power spectrum has  $1/f^\alpha$  behavior<sup>27</sup>. In what follows we describe the detrimental effects they produce and the limitations they determine.

The efficiency of the protocol versus stray detunings is shown in Fig. 4. The colour map shows  $P_1(t)$  for  $\Gamma_2 = 0$  at the end of the protocol,  $t = t_f$ . Lines refer to finite  $\Gamma_2 = 1/T$ , which determines a reduced value of  $P_1(t_f)$  since a nonvanishing population  $P_2(t)$  would decay outside the system. It is seen that the efficiency is large in a whole region around the center of the plot (absence of fluctuations,  $\tilde{\delta}_s = \tilde{\delta}_p = \tilde{\delta} = 0$ ), showing the stability of the protocol. The failure of cSTIRAP in the region of larger detunings is analyzed in the App. C. Here we mention that in the first and in the third quadrants of Fig. 4 failure is due to “bad projection” errors, i.e. the system may evolve along an adiabatic linkage leading to a wrong target state. Instead deep in the second quadrant the problem is “bad adiabaticity” due to an insufficient pump-induced two-photon avoided crossing.

Concerning sensitivity to  $\tau$ , notice that the convenient delay is implicitly set by the choice of  $\Omega_p(t)$  being maximal at the second crossing time, Eq.(7). We have checked that in these conditions the protocol is stable against deviations from the delay and the detailed pulse shape used in this work, provided they are not too large. Moreover it is worth stressing that the protocol we propose in

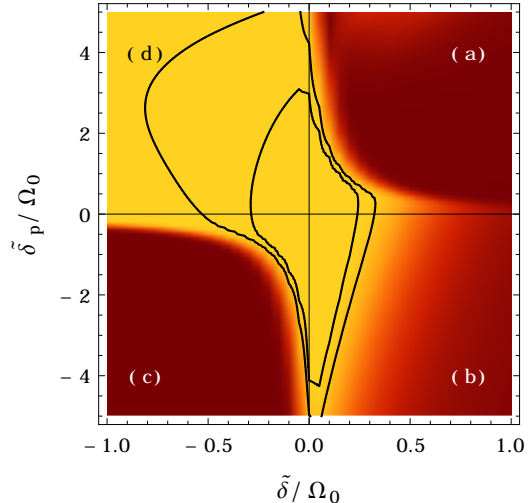


FIG. 4. (color online) The color map describes the efficiency of ideal cSTIRAP, with  $\Gamma_2 = 0$  vs fluctuations of the detunings. In the brightest area we have  $P_1(t_f) > 0.9$ . Lines refer to  $\Gamma_2 = 1/T$  and delimit the  $P_1(t_f) > 0.9$  (most inner region) and the  $P_1(t_f) > 0.8$  areas. We use the same parameters as in Fig. 2(b), which guarantee that in absence of fluctuations,  $\tilde{\delta}_s = \tilde{\delta}_p = \tilde{\delta} = 0$ , adiabaticity of the protocol is strong. The extension of the regions of large efficiency determines the single-photon linewidths (in this case  $\Delta\tilde{\delta}_s$ ) and the two-photon linewidth  $\Delta\tilde{\delta}$ .

the “ideal” detunings case, while being physically satisfactory, is not an optimal solution in the mathematical sense. Therefore we expect further improvement by tackling the problem with Optimal Control Theory.

## V. DECOHERENCE

A further important source of errors in STIRAP is decoherence<sup>21</sup>, especially in solid-state artificial atoms. We discuss some qualitative aspect in this section. A key asset of conventional STIRAP is that while spontaneous decay from  $|2\rangle$  may be large (decay time larger than the duration of the protocol), the phenomenon is supposed to have small impact as long as  $|2\rangle$  is depopulated. This holds true also for cSTIRAP, as seen from the results for  $\Gamma_2 \neq 0$  presented in the last Section. Markovian dephasing in STIRAP has been studied in detail<sup>30</sup> and its detrimental effect, namely leakage from the trapped subspace due to the weakening of destructive interference phenomenon, has been elucidated. It has been shown that strong Markovian dephasing is tolerated, as long as it does not affect the two levels of the trapped subspace. More complete studies of the effects of quantum noise in driven systems have pointed out that in solid state implementations of three-level artificial atoms the main effect is due to decay processes within the trapped subspace<sup>21</sup>. Other decoherence channels emerging in the Born-Markov approximation, namely the relation of rates

to the detailed spectral density of the environment<sup>31</sup> and the possible drive-induced absorption<sup>21</sup>, are less relevant.

On the other hand, unlike their natural counterpart, artificial atoms implemented by solid-state nanodevices suffer from low-frequency noise<sup>27</sup>. This drawback may be compensated by the ease of producing large couplings on chip, the tradeoff between protection and addressability being the central design issue. The effect of low-frequency noise in STIRAP has been discussed in Ref. 20, where its interplay with Markovian noise and the role of device design were also addressed<sup>21,32</sup>. The extension of this detailed analysis to cSTIRAP is beyond the scope of this paper, but general features pointed out in the above works together with the results of the last section, allow to draw a physical picture which can be used as a guide for device design.

We assume that low efficiency may be determined by decoherence leading to detrapping from the  $\{|0\rangle, |1\rangle\}$  subspace and by failures of the adiabatic approximation also leading to unwanted population of  $|2\rangle$ . The simplest model encompassing these main features is to account for decay of  $|2\rangle$  in a continuum due to quantum noise ( $\Gamma_2$ ) and to account for dephasing as due to low-frequency (classical) fluctuations of relevant parameters. That is we consider the Hamiltonian Eq.(1) supplemented by the non-Hermitian term appearing in Eq.(10), and let  $\delta_k(t) \rightarrow \delta_k(t) + \tilde{\delta}_k(t)$ , for  $k = s, p$ , and  $\Omega_k(t) \rightarrow \Omega_k(t) + \tilde{\Omega}_k(t)$ , where  $\tilde{\delta}_k(t)$  and  $\tilde{\Omega}_k(t)$  are classical stochastic processes. In artificial atoms such fluctuations stem physically from noisy external bias fields, which induce fluctuations of the energy splittings of the device (determining  $\tilde{\delta}_k$ 's) and of the operator coupling to the field (yielding  $\tilde{\Omega}_k$ 's). The efficiency is obtained by averaging over such fluctuations  $P_1(t|\{\tilde{\delta}_k\}, \{\tilde{\Omega}_k\})$ , at the end of the protocol. In cases of interest, as for  $1/f$  noise, the average can be estimated in the quasistatic (or static-path) approximation<sup>26,27</sup>. It amounts to substitute stochastic processes by random variables with a suitable Gaussian distribution, which physically accounts for sample to sample fluctuations of parameters. Results of the last section suggest that stray  $\tilde{\Omega}_k$ 's hardly affect the efficiency, whereas the effect of the distribution of  $\tilde{\delta}_k$ 's can be important. This effect can be read off in Fig.4, which shows that for reasonably small fluctuations there is a region where still large efficiencies are allowed. Successful cSTIRAP requires that fluctuations of energy levels (i.e. detunings) are smaller than the linewidths. In analogy with the analysis of Ref 21 we expect that the condition of large efficiency depends on the bandstructure of the device at the bias point. Indeed depending on the device and on the noise source, fluctuations of the two splittings (detunings) are either correlated or anticorrelated<sup>32</sup>, namely they are described by lines with positive or negative slope in Fig. 4. A figure of merit is the ratio  $\delta_{\frac{1}{2}}/\sigma_\delta$  between the two-photon linewidth of STIRAP, corresponding to the width of the large efficiency region in the proper direction in Fig. 4, and the variance  $\sigma_\delta$  of the fluctuations of the two-photon detuning.

## VI. CONCLUSIONS

In this paper we have proposed a new protocol which extends conventional STIRAP. Coherent population transfer is achieved with reduced available control, namely one of the field is kept always on. This procedure is suited for applications in artificial atoms and can be advantageous in integrated atom-cavity systems architectures, where couplings to quantized modes are implemented by non-switchable hardware<sup>12</sup>, and may be manipulated in this way for applications to microwave quantum photonics<sup>13</sup>. In this respect it may be useful that cSTIRAP can be repeated cyclically since population histories are invariant when  $\delta_k \rightarrow -\delta_k$ , allowing the protocol to work as well in the reverted detunings configuration.

The protocol leverages on the fact that in the microwave realm external fields have a phase which can be usually controlled better than for sources at optical frequencies. In particular frequency can be modulated more accurately allowing direct time-dependent control of the detunings, instead of the induced Stark shifts used in genuine atomic systems<sup>1</sup>. Moreover in solid-state artificial atoms, e.g. superconductor based, detunings can be independently modulated by external voltages and fluxes.

Manipulation of detunings is the basis of other coherent transfer protocols like RCAP<sup>29</sup>. The essential difference between standard RCAP and cSTIRAP is that, owing to the fact that the Stokes field is always-on, our protocol involves a dressed state in the AP phase (see Sec. III), whereas in the former AP occurs between bare states. Therefore while in RCAP the avoided crossing is due to the two-photon coupling of two far detuned dispersively coupled fields, in cSTIRAP AP takes place via destructively interfering *resonant* fields. This renders more robust the protocol, which achieves large efficiency for rather small pulse duration. On the other hand the analogy with RCAP, as well as the discussion of Sec. V, suggests that also cSTIRAP may be resilient to phase noise and to low-frequency noise in nanocircuits offering advantages in quantum state processing with artificial atoms<sup>19</sup>.

STIRAP is also the basis of other protocols as preparation of superpositions<sup>1</sup>, transfer of wavepackets<sup>33</sup>, manipulation of photons and quantum gates<sup>19</sup>, with still unexplored potentialities for quantum information and quantum control. Therefore demonstration of cSTIRAP is a benchmark for a class of multilevel advanced control protocols in artificial atoms.

### Appendix A: Adiabatic elimination of state $|2\rangle$

In order to estimate the population of  $|2\rangle$  we start from the usual adiabatic elimination in the bare basis. The Schrödinger equation  $i\partial_t|\psi\rangle = H|\psi\rangle$ , with the Hamiltonian Eq.(1), is written for the components of



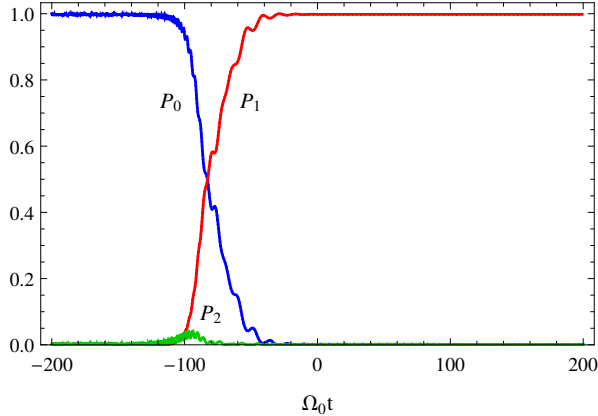


FIG. 5. (color online) Population histories for  $\Omega_p(t) =: \Omega_0, \Omega_0 T = 40, h_\delta = 10, \kappa_\delta = 1.2, \kappa = 1$  and  $\tau_{ch} = 0.6T$ .

$|\psi\rangle := \sum_{i=0}^2 c_i |i\rangle$ . Assuming  $\dot{c}_2 \simeq 0$  one finds

$$c_2 = -\frac{\Omega_p c_0 + \Omega_s c_1}{2\delta_p} \quad (\text{A1})$$

This expression of  $c_2$  is substituted in the Schrödinger equation yielding a two-state problem governed by the effective Hamiltonian

$$H_2(t) = \begin{bmatrix} -\frac{\Omega_p^2}{4\delta_p} & -\frac{\Omega_s \Omega_p}{4\delta_p} \\ -\frac{\Omega_s \Omega_p}{4\delta_p} & \delta - \frac{\Omega_s^2}{4\delta_p} \end{bmatrix} \quad (\text{A2})$$

Now assuming the validity of the adiabatic approximation,  $c_0$  and  $c_1$  are approximately given by the instantaneous eigenvectors of  $H_2(t)$ . In particular we consider the state corresponding to the preparation  $|\psi(t_i)\rangle = |0\rangle$ , and we can estimate  $P_2 = |c_2|^2$  from Eq. (A1). The analytic result is shown in Fig. 2(b), thin solid line in the inset, and it yields good agreement with the numerical curve. The analytic expression, though easy attainable, is cumbersome. Insight in the parametric dependence can be gained by evaluating leakage at  $t = t_c$ :

$$P_2(t_c) = \frac{\kappa_\delta - 1}{\kappa_\delta} \frac{(\kappa - \sqrt{\kappa^2 + 4})^2}{4 + (\kappa + \sqrt{\kappa^2 + 4})^2}$$

which is Eq. (8). We remind that adiabatic elimination yields coarse grained amplitudes and it is a priori enforced by large single-photon detunings. Remarkably the result obtained from Eq.(A1) is accurate for the whole procedure, even if in part of the protocol the condition  $\delta_p \gg \Omega_k$  is not met. This is due to the fact that the population of  $|2\rangle$  is always small, either because the regime is dispersive or because there is destructive interference.

Corrections in the regime where  $\delta_p(t) \lesssim \Omega_p, \Omega_s$  can be fully taken into account if adiabatic elimination is carried in the representation of the Stokes eigenstates. We write the Hamiltonian Eq.(1) in the basis  $\{|0\rangle, |s_+\rangle, |s_-\rangle\}$ , given by  $|s_\pm\rangle = a_1^\pm |1\rangle + a_2^\pm |2\rangle$ . By expressing  $|\psi\rangle = c_0 |0\rangle + c_+ |s_+\rangle + c_- |s_-\rangle$  and assuming

$\dot{c}_- \simeq 0$ , we obtain  $c_- = -(\Omega_-/2s_-)c_0$ , where  $\Omega_\pm = \Omega_p [1 + 4(\delta - s_\mp/\Omega_0)^2]^{-1/2}$ . Substituting the Ansatz for  $c_-$  into the Schrödinger equation yields an effective  $2 \times 2$  Hamiltonian, which in the  $\{|0\rangle, |s_+\rangle\}$  basis reads:

$$H_{2s} = \begin{bmatrix} -\frac{\Omega_-^2}{4s_-} & -\frac{\Omega_+}{2} \\ -\frac{\Omega_+}{2} & s_+ \end{bmatrix} \quad (\text{A3})$$

which yields the leakage to  $|2\rangle$  in the form

$$P_2 \simeq \left| \frac{\Omega_+}{2s_-} c_0 a_2^- + c_+ a_2^+ \right|^2 \quad (\text{A4})$$

As it is seen from Fig. 2(b) (dashed line) the result reproduces the numerical solution, but it does not yield a figure of merit as simple as Eq. 8.

## Appendix B: Always-on pump field

We can seek for a protocol dual to the always-on Stokes field by making the following substitutions,  $t_c \rightarrow -t_c$ ,  $\delta_p \rightleftharpoons \delta_s$ ,  $\Omega_p \rightleftharpoons \Omega_s$ . The population histories are shown in Fig. 5 and differ somehow from those of Sec.II. The point is that the system is prepared in  $|0\rangle$ , which in this case is not an exact eigenstate of the initial Hamiltonian. As a consequence Rabi oscillations of small amplitude appear in both  $P_0$  and  $P_2$ . They can be substantially reduced by increasing the initial value of the pump detuning. Stray population may appear in the intermediate state  $|2\rangle$  also due to adiabatic population transfer at the avoided crossing, and can be minimized by adjusting parameters as suggested by Eq. 8.

## Appendix C: Failure of STIRAP at large detunings

We now analyze the dynamics in the regions of Fig. 4 where cSTIRAP fails. As mentioned in Sec. IV when energy levels have infinite lifetime, failure of the protocol is due to two kind of errors, namely "bad adiabaticity" and "bad projection"<sup>3</sup>. While in the former case, the protocol fails because the avoided crossing produced by the fields is insufficient to guarantee adiabaticity, in the latter case the system is projected onto the wrong eigenstate of the Hamiltonian. Errors mainly occur during the AP near the point at  $t = t_c$  where Stokes eigenstates cross. An efficient protocol requires for the probabilities of Landau-Zener transitions between such states that  $\gamma_{0 \rightarrow s_-} \ll 1$  and  $1 - \gamma_{0 \rightarrow s_+} \ll 1$ , which is not always met for finite stray detunings.

A qualitative picture of how cSTIRAP possibly fails due to stray detunings is offered by the patterns of the instantaneous eigenvalues of the full and of the Stokes Hamiltonians, in the darker regions of the three (a-c) quadrants of Fig. 4. Examples of these patterns are plotted in Fig. 6(a-c).

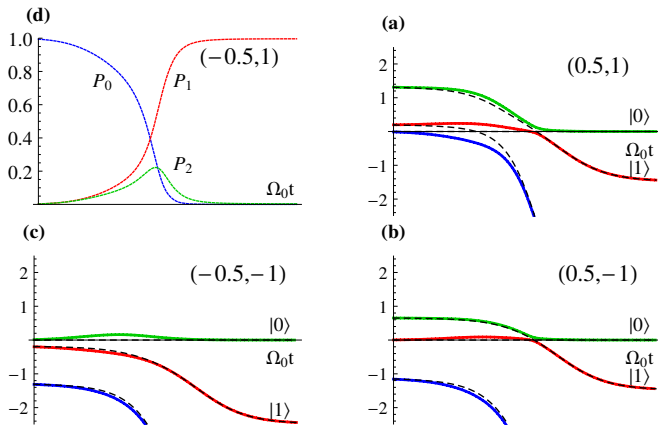


FIG. 6. (color online) (a-c) Instantaneous eigenvalues of the Stokes (dashed lines) and complete (solid lines) Hamiltonians, in the dark regions of quadrants (a-c) of Fig. 4, in units of  $\Omega_0$ . (d) Population histories corresponding to quadrant (d) of Fig. 4 for  $\Gamma_2 = 0$ , showing that, even if  $P_1(t_f)$  is nearly one, the protocol suffers of large transient population of  $|2\rangle$  (green line). In each panel the label  $(\tilde{\delta}/\Omega_0, \tilde{\delta}_p/\Omega_0)$  indicates the value of the stray detunings.

In the region deep in quadrant (a) of Fig. 4 detunings are such that the first crossings of the Stokes eigenenergies occurs *at positive times*, i.e. when  $\Omega_p$  is already on [Fig. 6(a)]. Therefore  $|0\rangle$  and  $|s_-\rangle$  mix, originating a sort of initial “bad projection” error. Then the sub-

sequent swap  $|s_-\rangle \rightarrow |2\rangle$  leads to a wrong target state. Deep in quadrant (b), the protocol suffers from a sort of final “bad projection” error: the second crossing occurs *at negative times*, where  $\Omega_p \approx 0$  and the correspondent transition becomes diabatic. This yields  $|\psi(t)\rangle \approx |0\rangle$  at all times<sup>34</sup>. Deep in quadrant (c) cSTIRAP fails when the configuration of detunings renders the pump-induced avoided crossing insufficient. In this case the problem is “bad adiabaticity”, Zener tunneling inducing unwanted transitions to the state adiabatically evolving towards  $|0\rangle$ .

Finally, deep in the quadrant (d) the configuration of detunings is such that the two “mixing” phases of the protocol are inverted. Indeed the Stokes-induced AT splitting becomes relevant only *after* the second crossing, which in the ideal case would have produced the two-photon AP. Therefore  $\Omega_p$  partially injects population into  $|2\rangle$ . At later times, in the Stokes-AT phase, this population is swapped to  $|1\rangle$ . Although the final state is correct (cf. the large efficiency in Fig. 4), in the presence of decay  $\Gamma_2 \neq 0$ , occupation of  $|2\rangle$  at intermediate times suppresses the efficiency [see Fig. 6(d) and the solid lines of Fig. 4].

## ACKNOWLEDGMENTS

This work was partially supported by MIUR through Grant. No. PON02\_00355\_3391233, “Tecnologie per l’ENERGia e l’Efficienza enerGETICa - ENERGETIC”. A. D’Arrigo acknowledges partial support by Centro Siciliano di Fisica Nucleare e Struttura della Materia.

\* gfalci@dmfci.unict.it

- <sup>1</sup> N. V. Vitanov, B. W. S. T. Halfmann, and K. Bergmann, *Annu. Rev. Phys. Chem.* **52**, 763 (2001).
- <sup>2</sup> M. Nielsen and I. Chuang, *Quantum Computation and Quantum Information* (Cambridge Univ. Press, Cambridge, 2010).
- <sup>3</sup> N. Vitanov, M. Fleischhauer, B. Shore, and K. Bergmann, *Adv. in At. Mol. and Opt. Phys.* *Advances In Atomic, Molecular, and Optical Physics*, **46**, 55 (2001).
- <sup>4</sup> K. Bergmann, H. Theuer, and B. Shore, *Rev. Mod. Phys.* **70**, 1003 (1998).
- <sup>5</sup> A. Kuhn, M. Hennrich, and G. Rempe, *Phys. Rev. Lett.* **89**, 067901 (2002).
- <sup>6</sup> M. Mücke, J. Bochmann, C. Hahn, A. Neuzner, C. Nölleke, A. Reiserer, G. Rempe, and S. Ritter, *Phys. Rev. A* **87**, 063805 (2013).
- <sup>7</sup> J. Q. You and F. Nori, *Nature* **474**, 589 (2011).
- <sup>8</sup> J. Klein, F. Beil, and T. Halfmann, *Phys. Rev. A* **78**, 033416 (2008).
- <sup>9</sup> J. Clarke and F. K. Wilhelm, *Nature* **453**, 1031 (2008).
- <sup>10</sup> I. Buluta, S. Ashhab, and F. Nori, *Rep. Prog. Phys.* **74**, 104401 (2011).
- <sup>11</sup> M. Devoret and R. Schoelkopf, *Science* **339**, 1169 (2013).
- <sup>12</sup> R. J. Schoelkopf and S. M. Girvin, *Nature* **451**, 664 (2008).

- <sup>13</sup> Y. Nakamura and T. Yamamoto, *IEEE Photonics Journal* **5** (2013).
- <sup>14</sup> T. Niemczyk, F. Deppe, H. Huebl, F. Menzel, E.P. and Hocke, M. Schwarz, J. Garcia-Ripoll, D. Zueco, T. Hümmer, E. Solano, A. Marx, and R. Gross, *Nature Physics* **6**, 772776 (2010).
- <sup>15</sup> K. V. R. M. Murali, Z. Dutton, W. D. Oliver, D. S. Crankshaw, and T. P. Orlando, *Phys. Rev. Lett.* **93**, 087003 (2004).
- <sup>16</sup> Y. X. Liu, J. Q. You, L. F. Wei, C. P. Sun, and F. Nori, *Phys. Rev. Lett.* **95** (2005), 10.1103/PhysRevLett.95.087001.
- <sup>17</sup> J. Siewert, T. Brandes, and G. Falci, *Optics Communications* **264**, 435 (2006), quantum Control of Light and Matter - In honor of the 70th birthday of Bruce Shore.
- <sup>18</sup> J. Siewert, T. Brandes, and G. Falci, *Phys. Rev. B* **79**, 024504 (2009).
- <sup>19</sup> L. F. Wei, J. R. Johansson, L. X. Cen, S. Ashhab, and F. Nori, *Phys. Rev. Lett.* **100**, 113601 (2008).
- <sup>20</sup> G. Falci, M. Berritta, A. Russo, A. D’Arrigo, and E. Paladino, *Phys. Scr.* **T151** (2012).
- <sup>21</sup> G. Falci, A. La Cognata, M. Berritta, A. D’Arrigo, E. Paladino, and B. Spagnolo, *Phys. Rev. B* **87**, 214515 (2013).
- <sup>22</sup> M. A. Sillanpää, J. Li, K. Cicak, F. Altomare, J. I. Park, R. W. Simmonds, G. S. Paraoanu, and P. J. Hakonen,



- Phys. Rev. Lett. **103**, 193601 (2009).
- <sup>23</sup> M. Baur, S. Filipp, R. Bianchetti, J. M. Fink, M. Göppl, L. Steffen, P. J. Leek, A. Blais, and A. Wallraff, Phys. Rev. Lett. **102**, 243602 (2009).
- <sup>24</sup> J. Li, G. Paraoanu, K. Cicak, F. Altomare, J. Park, R. Simmonds, M. Sillanpää, and P. Hakonen, Scientific Reports 2 **Art. num. 645** (2012).
- <sup>25</sup> W. R. Kelly, Z. Dutton, J. Schlafer, B. Mookerji, T. A. Ohki, J. S. Kline, and D. P. Pappas, Phys. Rev. Lett. **104**, 163601 (2010).
- <sup>26</sup> G. Falci, A. D'Arrigo, A. Mastellone, and E. Paladino, Phys. Rev. Lett. **94**, 167002 (2005).
- <sup>27</sup> E. Paladino, Y. Galperin, G. Falci, and B. Altshuler, Rev. Mod. Phys. **86**, 361 (2014).
- <sup>28</sup> C. Cohen-Tannoudji, Kosmos, revue de la Socit Sudoise de Physique (2009).
- <sup>29</sup> I. R. Solá, V. S. Malinovsky, B. Y. Chang, J. Santamaria, and K. Bergmann, Phys. Rev. A **59**, 4494 (1999).
- <sup>30</sup> P. A. Ivanov, N. V. Vitanov, and K. Bergmann, Phys. Rev. A **70**, 063409 (2004).
- <sup>31</sup> E. Geva, R. Kosloff, and J. Skinner, J. Chem. Phys. **102**, 8541 (1995).
- <sup>32</sup> P. G. Di Stefano, E. Paladino, A. D'Arrigo, B. Spagnolo, and G. Falci, Romanian J. Phys. (2015).
- <sup>33</sup> P. Král, I. Thanopoulos, and M. Shapiro, Rev. Mod. Phys. **79**, 53 (2007).
- <sup>34</sup> In describing the behaviour in the first and third quadrant we rely on the distinction between negative and positive times. This asymmetry roots from the choice of switching on  $\Omega_p(t)$  at slightly positive times.